Pyroelectric and Dielectric Properties of Ferroelectric Films With Interposed Dielectric Buffer Layers

Y. Espinal,[1] M. T. Kesim,[1] I. B. Misirlioglu,[2] S. Trolier-McKinstry,[3]
J. V. Mantese,[4] and S. P. Alpay [1,5,a]

[1] *Department of Materials Science and Engineering and Institute of Materials Science University of Connecticut, Storrs, CT 06269, USA*

[2] *Faculty of Engineering and Natural Sciences Sabanci University, Tuzla/Orhanli 34956 Istanbul, Turkey*

[3] *Department of Materials Science and Engineering and Materials Research Institute, Pennsylvania State University, University Park, PA 16802, USA*

[4] *United Technologies Research Center, East Hartford, USA*
[5] *Department of Physics, University of Connecticut, Storrs, CT 06269, USA*

Abstract

We theoretically investigate dielectric and pyroelectric properties of ferroelectric films with linear dielectric buffer layers. Computations were carried out for multilayers consisting of $PbZr_{0.2}Ti_{0.8}O_3$ with Al_2O_3, SiO_2, Si_3N_4, HfO_2 and TiO_2 buffers on metalized Si. We show that the dielectric and pyroelectric properties of such multilayers are not significantly diminished by the presence of the buffer layer compared to their homogeneous ferroelectric counterparts. Indeed, stacked multilayer ferroelectric films with dielectric buffers can be used to not only provide high electric field breakdown strength films, but may be designed to optimize pyroelectric and dielectric properties of ferroelectric multilayer films.

Keywords: pyroelectric, electrocaloric, ferroelectrics, multilayers

[a] Corresponding author, e-mail: p.alpay@ims.uconn.edu

The origin of the dielectric (DE) and pyroelectric properties of ferroelectric (FE) materials and their thin film embodiments have been well understood for several decades. Moreover, their dependencies upon: crystal structure, temperature, applied electric field and stress, thickness, etc., have been studied extensively both experimentally and theoretically.[1–7] Most recently, however, the behavior of this class of thin film materials at very high fields, $\geq$100 MV/m, has become of interest for their enhanced electrocaloric response.[8]

Non-polymeric bulk FE materials cannot easily sustain electric fields exceeding ~1MV/m due to the density and hence aggregated number of defects within the materials.[8,9] Thin film FEs, however, when deposited upon suitable substrates have been shown to support electric fields of much greater magnitude due to their improved crystallinity, smaller number of crystalline and electronic defects, and high densities within the associated volume element comprising the film.[10–12] Mechanisms of high field failure and current leakage fall into one of the two following categories: bulk-limited and interface-limited conduction. Of all the possible leakage mechanisms, the three most commonly observed in FE perovskite oxides are interface-limited Schottky emission, bulk-limited space-charge-limited conduction and bulk-limited Poole-Frenkel emission.[13,14] Thus, even thin film FE often cannot easily sustain repeated high electric field cycling.

It has been, however, shown experimentally that adding a DE buffer layer will improve leakage and loss characteristics of ferroelectric devices under high field.[15–18] For example, $Ba_xSr_{1-x}TiO_3$ (BST) films grown on sapphire with a 9 nm $SrTiO_3$ (STO) buffer layer has a lower leakage current (~$1x10^{-8}$ A/cm^2 at 0 V) compared to a BST monolayer with no buffer layer (~$1x10^{-7}$ A/cm^2 at 0 V)[19]; and, therefore, motivate adoption of solutions taken from the integrated circuit (IC) and MEMS device community to address such problems. Indeed, it has

long been known that interposing a high quality DE (e.g., Si_3N_4, or similar) between an inferior material of lesser electric field breakdown strength can substantially improve the overall field strength of a multilayer.[20] However, it is a matter of rudimentary physics that the DE properties of such a multilayer will often be dependent upon the material with the smaller relative permittivity – subject to geometrical film thickness considerations. It is this latter proviso that we explore theoretically in this paper; namely the role of an interposed thin film DE on the pyroelectric and DE properties of the multilayer. To do this, we use a non-linear thermodynamic model and investigate the room temperature (RT=25°C) DE and pyroelectric properties of FE/DE bilayers. It is known that FE multilayers or compositionally graded structures exhibit unusual properties that have been attributed to elastic and electro-mechanical interactions.[21–23] A thermodynamic analysis carried out for STO/$BaTiO_3$ (BTO) bilayers has revealed the presence of a critical relative thickness of STO at which a large DE response is expected.[21] This anomaly is explained through the presence of internal (depolarizing) fields that suppress ferroelectricity at a critical volume fraction of STO. In this study we use a similar methodology to investigate the pyroelectric properties of $Pb(Zr_{0.2}Ti_{0.8})O_3$ PZT(20/80) as a prototypical FE and several distinct materials for the DE buffer layers including alumina (Al_2O_3), silica (SiO_2), silicon nitride (Si_3N_4), hafnia (HfO_2), and titania (TiO_2). We show here that the pyroelectric response is marginally affected by the presence of buffer layers below a critical thickness. Lastly, we find that "designed" multilayer FE films with buffer layers tailored to critical thicknesses can be used to optimize properties of FE films.

Consider a (001)-textured, mono-domain PZT 20/80 film on a Si substrate with linear DE buffer layers schematically shown in Fig. 1(a) with the linear DE being Al_2O_3 as an example. We

assume that the films are deposited at a growth temperature (T_G) of 550°C and then cooled to RT. The non-equilibrium excess free energy of such a system in the FE state can be expressed as:

$$G = (1-\alpha)\cdot G_1(P_1, T, u_T, E) + \alpha \cdot G_2(P_2, E) + \frac{1}{2}\alpha(1-\alpha)\frac{1}{\varepsilon_0}(P_1 - P_2)^2 + \frac{G_S}{h} \quad (1)$$

where α is the layer fraction of the buffer layer (defined as the thickness of the buffer layer divided by the total film thickness), u_T is the in-plane thermal strain due to thermal expansion mismatch between PZT and Si ($\Delta\alpha=\alpha_{PZT} - \alpha_{Si}$) and given by $u_T = \int_T^{T_G} \Delta\alpha dT$. The third term in Eq. (1) is the contribution due to interlayer coupling. G_i are the uncoupled free energies of each layer and given by:

$$G_1(P_1, T, u_T, E) = G_{0,1} + \tilde{a}_1 P_1^2 + \tilde{b}_1 P_1^4 + c_1 P_1^6 + \frac{u_T^2}{S_{11} + S_{12}} - EP_1 \quad (2)$$

$$G_2(P_2, E) = \frac{P_2^2}{2\varepsilon_0 \varepsilon_{R,2}} - EP_2 + G_{EL} \quad (3)$$

where $\tilde{a}_i$, $\tilde{b}_i$, and c_i are the DE stiffness coefficients of the FE and S_{ij} are the elastic compliances at constant polarization, for which values were obtained from the literature.[24–27] The modified coefficients $\tilde{a}_i$ and $\tilde{b}_i$ in Eq. (2) read;

$$\tilde{a}_1 = a_1 - \frac{2Q_{12}}{S_{11} + S_{12}} u_T \quad \text{and} \quad \tilde{b}_1 = b_1 + \frac{Q_{12}^2}{S_{11} + S_{12}} \quad (4)$$

where Q_{ij} are the cubic electrostrictive coefficients of PZT. ε_0 is the permittivity of vacuum and ε_{R2} is the DE constant of the buffer layer (layer 2). We note that layer 2 is a linear DE and the elastic energy G_{EL} in Eq. (3) is not polarization dependent. The equilibrium polarizations P_1^0 and P_2^0 are obtained from Eqs. (2), (3) and from the equations of state $\partial G/\partial P_1=0$ and $\partial G/\partial P_2=0$.

Pyroelectric and DE properties are then computed from the relevant Maxwell's relations such that:

$$p = \frac{dP_S}{dT} + \int_0^E \left(\frac{\partial \varepsilon}{\partial T}\right)_E dE \tag{5}$$

$$\langle \varepsilon_R \rangle = \frac{1}{\varepsilon_0}\frac{d\langle P \rangle}{dE} = \frac{1}{\varepsilon_0}\left[(1-\alpha)\frac{dP_1^0}{dE} + \varepsilon \frac{dP_2^0}{dE}\right] \tag{6}$$

where $\langle P \rangle = (1-\alpha)P_1^0 + \alpha P_2^0$ is the average polarization. The second term in Eq. (5) is the DE contribution to the total pyroelectric response and it can be neglected for films in the polar FE state in the absence of external bias.[26]

Fig. 1(b) shows the average out of plane polarization of PZT 20/80 films for T_G=550°C as a function of Al_2O_3 layer fraction on platinum coated Si. The net polarization decreases rapidly with increasing thickness Al_2O_3 (with a zero spontaneous polarization, P_S) due to large polarization mismatch between the FE and DE layer. Specifically, at a critical thickness of only ~2% of the PZT; P_s is zero in the absence of a bias field. Application of an electric field to compensate for the polarization decay shifts the critical thickness to a larger value. Conversely, the average dielectric permittivity (ε_R) and pyroelectric, p, response of the composite structure gradually increases with increasing Al_2O_3 layer fraction as can be seen in Figs. 1(c) and 1(d). This seemingly counterintuitive result is related to two factors: electrostatic coupling between layers and a shift in the Curie temperature to lower temperatures as a result of the interfacial strain between the FE and the interposed DE layer. In this example, an abrupt change of spontaneous polarization at the critical buffer layer fraction increases ε_R for bulk PZT from 85 to 310 for structures with 1.00% Al_2O_3 interposed between a platinum coated films clamped on Si substrate with a growth temperature T_G=550°C. Fig. 1(d) plots the pyroelectric coefficient of

PZT-Al_2O_3 bilayers as a function of the buffer layer fraction. Adding a DE layer to PZT films drastically improves the pyroelectric properties. In this same example, a bilayer composed a PZT film with 1.00% Al_2O_3 shows a pyroelectric coefficient of 0.070 μC/cm^2 °C which is 80% higher than the value computed for PZT 20/80 monolayer on Si. Remarkably, these results run counter to approximations that describe DE bi-layers as capacitors in series.[28,29] Calculations for Si_3N_4 as the buffer layer yield similar results. For PZT with T_G=550^{o}C, the critical fraction of Si_3N_4 is 1.75%. This is because the bulk dielectric permittivity of Si_3N_4 and Al_2O_3 are similar (7 and 8, respectively). For a bilayer with Si_3N_4 fraction equal to 1.00%, the ε_R and the pyroelectric coefficients are ~360 and 0.078 μC/cm^2 °C. The above findings are consistent with the fact that active electrocaloric and pyroelectric thin film devices often have active FE layer thicknesses of ~1000 nm, whereas the thicknesses necessary to achieve high DE field breakdown strengths in interposed DE layers are often on the order of 1-10 nm, making these results encouraging for the next generation pyroelectric and electrocaloric devices.

Fig. 2 shows the relationship between DE and pyroelectric properties as a function of the buffer layer fraction for four different DEs. The configuration of bilayers with SiO_2, HfO_2 and TiO_2 is identical to the one shown in Fig. 1 (a). It is seen, that due to the polarization mismatch between the layers, a critical layer fraction exists at which both the pyroelectric coefficient and ε_R rapidly increase. For alumina, this critical fraction is about 1.95%. For SiO_2, Si_3N_4, HfO_2 and TiO_2 these layer fractions are approximately 1.10%, 1.75% 5.00%, and 20.40%, respectively. There is a direct relationship between the critical layer fraction and the DE constant, namely that materials with higher intrinsic permittivity more closely couple to the polarization, much as we might expect from our simple capacitor models in the absence of induced FE to DE phase transitions.

Fig. 3 plots the critical layer fraction as a function of relative DE permittivity of the DE buffer layer for titanium rich PZT compositions (which progressively shift the Curie temperature). Bulk DE permittivities for common DE materials are denoted on the top axis. The critical layer fraction increases with increasing bulk DE constant of the buffer layer. The DE constants of common DEs are marked on the top axis of Fig. 3. It is also noted that for PZT compositions with larger zirconium concentrations the critical layer fraction increases at a faster rate. For example, the critical layer fraction for a buffer layer with DE constant of 40 on PZT 0/100 ($PbTiO_3$) is 9.00% compared to PZT 40/60 for which it is about 4.50%. Consequently, control of thickness during deposition/growth and the choice of the buffer layer can be exploited to optimize the pyroelectric coefficient as well as the DE constant of the FE multilayer.

It should be noted that these calculations are carried out for monodomain films that are assumed to be perfectly (001)-aligned. PZT films grown on platinized Si substrates are predominantly (111) textured.[30] Therefore the polarization and pyroelectric vector components lie along [111] and hence the computed values are lowered for such films.[26,31] It is therefore necessary to find synthesis routes that will produce (001)-textured films to maximize the pyroelectric response of the films and having a buffer layer may help. Moreover, the interfacial energy due to polarization gradients at the interlayer interface is neglected in Eq. (1) when computing the equilibrium properties of the bilayers. This is a valid assumption provided that the individual layers that make up the multilayer are sufficiently thick. As seen in Fig. 3, the critical layer fraction is ~2.5% for a DE with κ_R=10. For a 100 nm-thick bilayer, the required thickness of the DE should therefore be ~2.5 nm for which the polarization distribution at the layer interface may have a substantial effect on the DE and pyroelectric properties.

To facilitate better thermal transport through a pyroelectric device, the substrates are back-etched to remove Si which is not a good thermal conductor.[32] This reduces the time coefficient of the detector and increases the figure of merit.[33,34] We have carried out computations for such a case where Si is assumed to be removed from the bilayer prior to growth/deposition. For a PZT 20/80 with an Al_2O_3 buffer layer with α=1.00% at T_G=550^{o}C, the DE constant and the pyroelectric coefficient (~145 and 0.054 μC/cm^2 °C) are actually lower than for bilayers on Si. This is related to the fact that thermal strains in PZT 20/80 may actually improve DE and electrothermal properties as shown in Kesim *et al.*[35] and Zhang *et al.*[25] by shifting the Curie temperature to RT.

Prior studies by the IC and MEMS community have shown that the DE strength of DE films may be increased nearly tenfold by interposing high breakdown strength DEs of 1-10 nm thickness.[20] Such works, together with the findings of this paper suggest that the performance of pyroelectric based energy conversion devices (thermal to electric and electric to thermal) could benefit from this approach. Specifically, it has been demonstrated that the field dependence of the temperature lifts attainable through the electrocaloric effect are power law of coefficient greater than 1. Hence, application and sustainment of fields >100MV/m significantly improve the temperature lifts produced from the materials now widely being studied in this active field of research.

FIGURE CAPTIONS

Figure 1: (Color online) (a) Schematic of PZT 20/80 film with Al_2O_3 buffer layer on Si. Room temperature (b) polarization, (c) small signal relative dielectric permittivity, and (d) pyroelectric coefficient curves of PZT 20/80 as a function of Al_2O_3 layer fraction for T_G=550°C on Si for E=0, 50, 100, 150, and 200 kV/cm.

Figure 2: (Color online) Pyroelectric coefficient and relative dielectric permittivity of PZT 20/80 as a function of (a) Al_2O_3, (b) SiO_2, (c) HfO_2, and (d) TiO_2 layer fractions for T_G=550°C on Si for E=0 kV/cm.

Figure 3: (Color online) Critical layer fraction of FE/DE bilayers as a function of the relative dielectric permittivity of the DE layer (T_G=550°C, E=0 kV/cm) for Ti-rich PZT compositions.

REFERENCES

[1] O.G. Vendik, L.T. Ter-Martirosyan, and S.P. Zubko, J. Appl. Phys. **84**, 993 (1998).

[2] C.L. Canedy, H. Li, S.P. Alpay, L. Salamanca-Riba, a. L. Roytburd, and R. Ramesh, Appl. Phys. Lett. **77**, 1695 (2000).

[3] S. Hoon Oh and H. Jang, Phys. Rev. B **62**, 14757 (2000).

[4] T.M. Shaw, S. Trolier-Mckinstry, and P.C. McIntyre, Annu. Rev. Mater. Sci. **30**, 263 (2000).

[5] T.R. Taylor, P.J. Hansen, B. Acikel, N. Pervez, R.A. York, S.K. Streiffer, and J.S. Speck, Appl. Phys. Lett. **80**, 1978 (2002).

[6] H.X. Cao, V.C. Lo, and W.W.Y. Chung, J. Appl. Phys. **99**, 024103 (2006).

[7] S.P. Beckman, L.F. Wan, J. a. Barr, and T. Nishimatsu, Mater. Lett. **89**, 254 (2012).

[8] M. Valant, A.-K. Axelsson, F. Le Goupil, and N.M. Alford, Mater. Chem. Phys. **136**, 277 (2012).

[9] M. Ožbolt, A. Kitanovski, J. Tušek, and A. Poredoš, Int. J. Refrig. **37**, 16 (2014).

[10] S.G. Yoon and A. Safari, Thin Solid Films **254**, 211 (1995).

[11] C.-R. Cho, W.-J. Lee, B.-G. Yu, and B.-W. Kim, J. Appl. Phys. **86**, 2700 (1999).

[12] J. Celinska, V. Joshi, S. Narayan, L. McMillan, and C. Paz de Araujo, Appl. Phys. Lett. **82**, 3937 (2003).

[13] G.W. Pabst, L.W. Martin, Y.-H. Chu, and R. Ramesh, Appl. Phys. Lett. **90**, 072902 (2007).

[14] S.K. Sahoo, D. Misra, D.C. Agrawal, Y.N. Mohapatra, S.B. Majumder, and R.S. Katiyar, J. Appl. Phys. **108**, 074112 (2010).

[15] A. Roy, A. Dhar, D. Bhattacharya, and S.K. Ray, J. Phys. D. Appl. Phys. **41**, 095408 (2008).

[16] V. Reymond, D. Michau, S. Payan, and M. Maglione, Ceram. Int. **30**, 1085 (2004).

[17] C.L. Sun, S.Y. Chen, M.Y. Yang, and A. Chin, J. Electrochem. Soc. **148**, F203 (2001).

[18] K.-J. Choi, W.-C. Shin, J.-H. Yang, and S.-G. Yoon, Appl. Phys. Lett. **75**, 722 (1999).

[19] M.W. Cole, E. Ngo, C. Hubbard, S.G. Hirsch, M. Ivill, W.L. Sarney, J. Zhang, and S.P. Alpay, J. Appl. Phys. **114**, 164107 (2013).

[20] S.S. Ahmed, J.P. Denton, and G.W. Neudeck, J. Vac. Sci. Technol. B **19**, 800 (2001).

[21] A.L. Roytburd, S. Zhong, and S.P. Alpay, Appl. Phys. Lett. **87**, 092902 (2005).

[22] A.M. Bratkovsky and A.P. Levanyuk, J. Comput. Theor. Nanos. **6**, 465 (2009).

[23] N.A. Pertsev, P.E. Janolin, J.-M. Kiat, and Y. Uesu, Phys. Rev. B **81**, 144118 (2010).

[24] N.A. Pertsev, A.G. Zembilgotov, and A.K. Tagantsev, Phys. Rev. Lett. **80**, 1988 (1998).

[25] J. Zhang, M.W. Cole, and S.P. Alpay, J. Appl. Phys. **108**, 054103 (2010).

[26] M.T. Kesim, J. Zhang, S. Trolier-McKinstry, J. V. Mantese, R.W. Whatmore, and S.P. Alpay, J. Appl. Phys. **114**, 204101 (2013).

[27] M.J. Haun, Z.Q. Zhuang, E. Furman, S.J. Jang, and L.E. Cross, Ferroelectrics **99**, 45 (1989).

[28] L.J. Sinnamon, R.M. Bowman, and J.M. Gregg, Appl. Phys. Lett. **78**, 1724 (2001).

[29] A.M. Bratkovsky and A.P. Levanyuk, Phys. Rev. B **63**, 132103 (2001).

[30] N.M. Shorrocks, A. Patel, M.J. Walker, and A.D. Parsons, Microelectron. Eng. **29**, 59 (1995).

[31] Q. Du, J. Li, W. Nothwang, and M.W. Cole, Acta Mater. **54**, 2577 (2006).

[32] W. Liu, J.S. Ko, and W. Zhu, Thin Solid Films **371**, 254 (2000).

[33] R.W. Whatmore, Rep. Prog. Phys. **49**, 1335 (1986).

[34] Z. Xu, D. Yan, D. Xiao, P. Yu, and J. Zhu, Ceram. Int. **38**, 981 (2012).

[35] M.T. Kesim, M.W. Cole, J. Zhang, I.B. Misirlioglu, and S.P. Alpay, Appl. Phys. Lett. **104**, 022901 (2014).

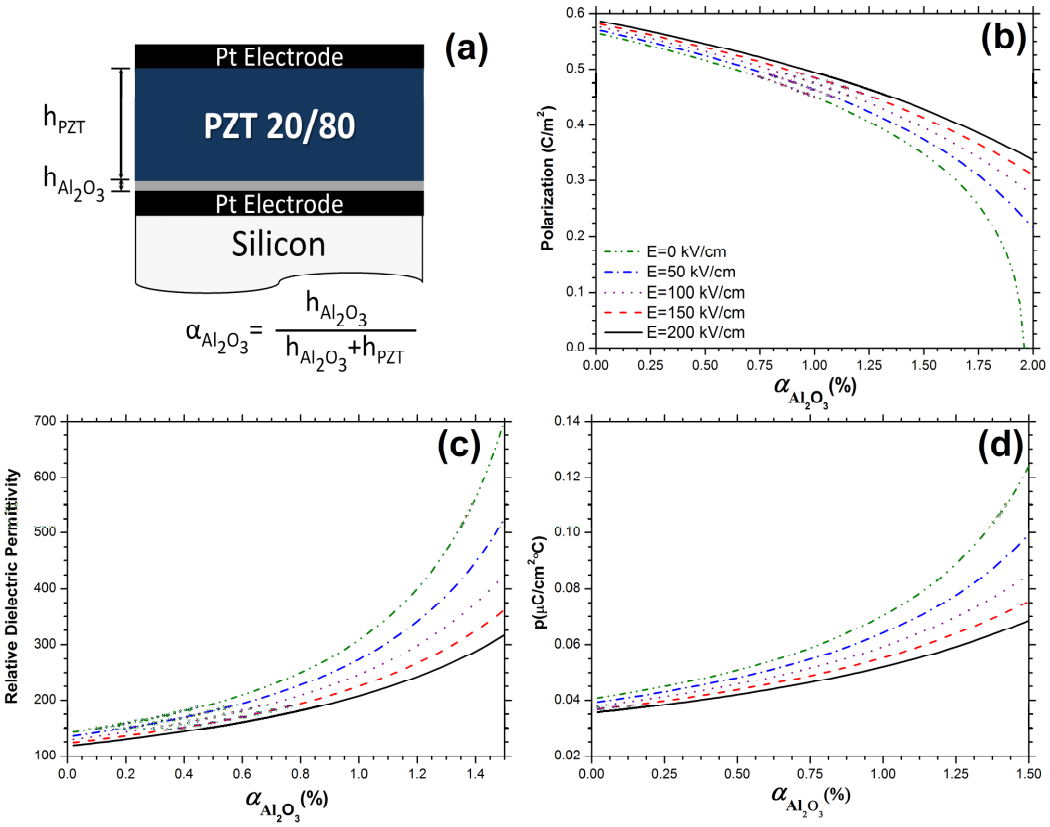
(a)
Pt Electrode
PZT 20/80
Pt Electrode
Silicon
h_{PZT}
$h_{Al_2O_3}$
$\alpha_{Al_2O_3} = \frac{h_{Al_2O_3}}{h_{Al_2O_3}+h_{PZT}}$
(b)
Polarization (C/m^2)
E=0 kV/cm
E=50 kV/cm
E=100 kV/cm
E=150 kV/cm
E=200 kV/cm
$\alpha_{Al_2O_3}$ (%)
(c)
Relative Dielectric Permittivity
$\alpha_{Al_2O_3}$ (%)
(d)
p(μC/cm^2·C)
$\alpha_{Al_2O_3}$ (%)

Figure 1

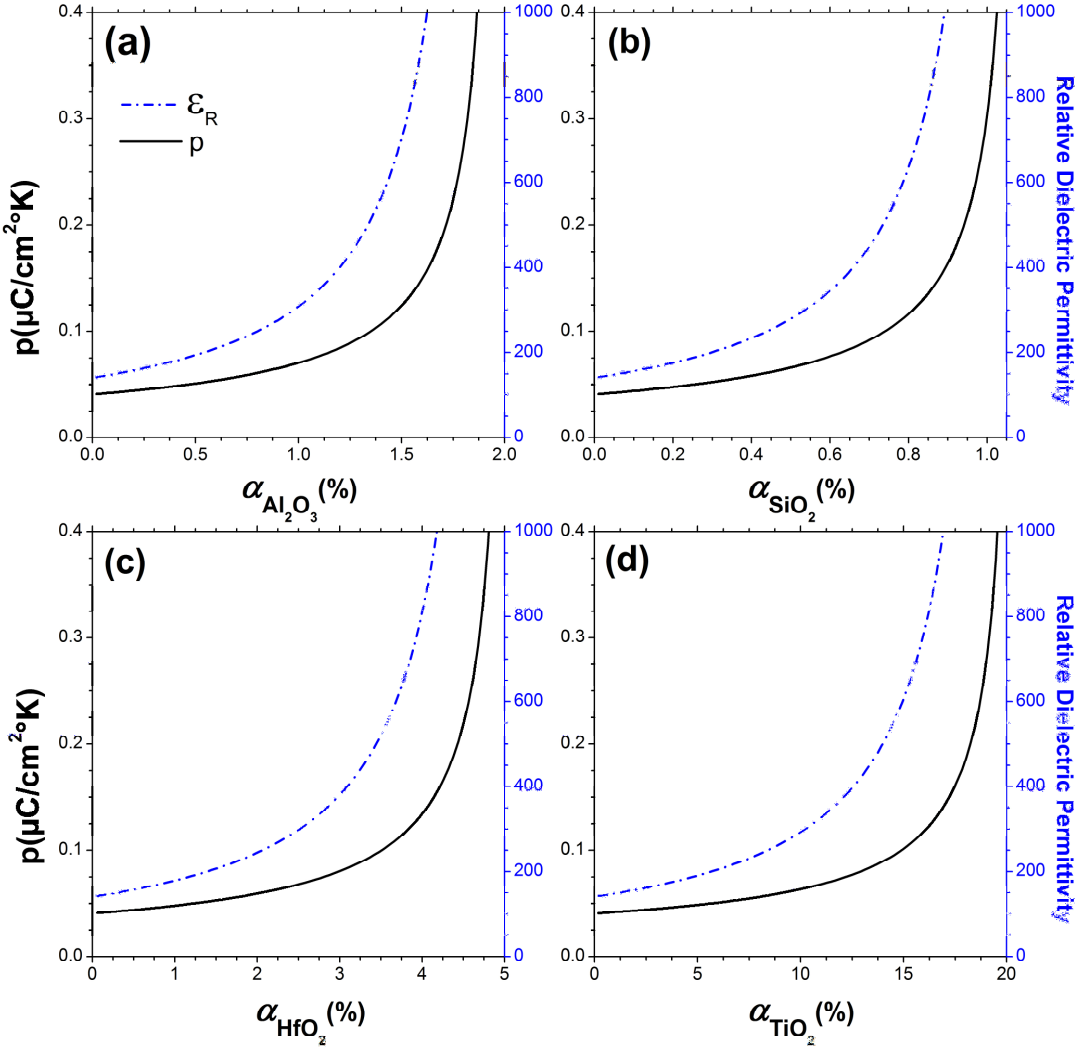
(a)
(b)
(c)
(d)
ε_R
p
p(μC/cm^2°K)
Relative Dielectric Permittivity
$\alpha_{Al_2O_3}$(%)
α_{SiO_2}(%)
α_{HfO_2}(%)
α_{TiO_2}(%)

Figure 2

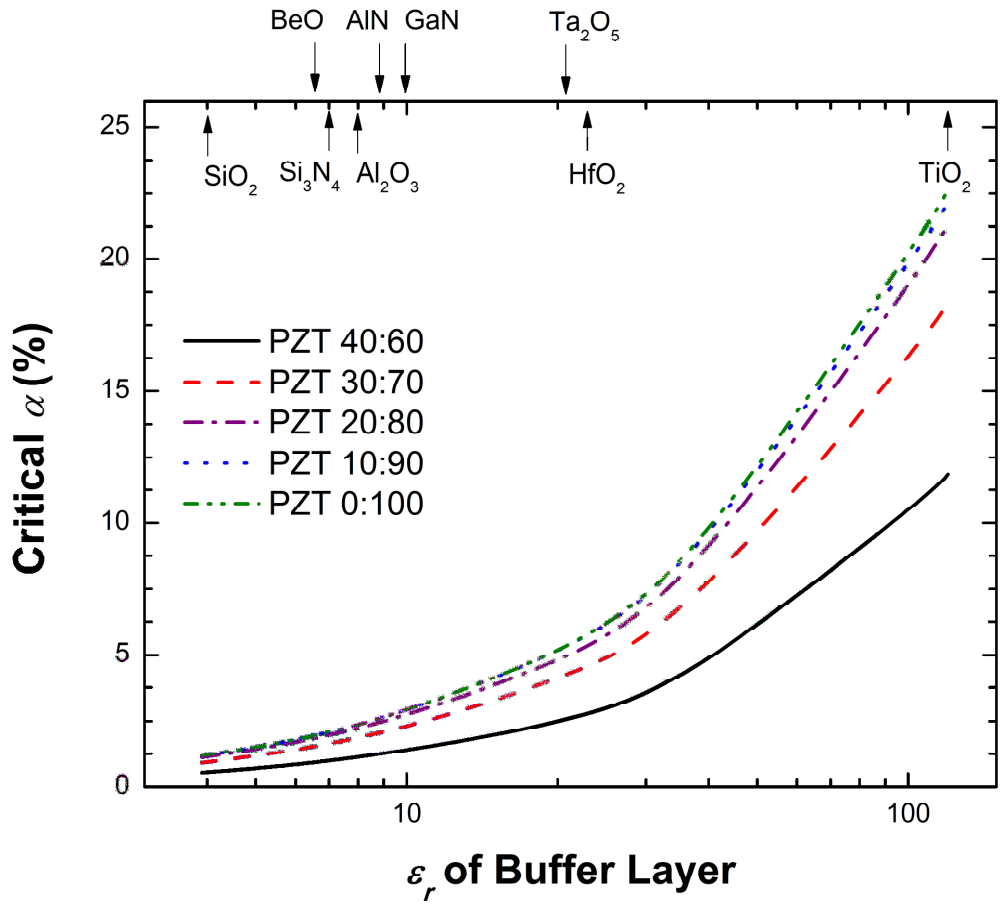
BeO
AlN
GaN
Ta_2O_5
SiO_2
Si_3N_4
Al_2O_3
HfO_2
TiO_2
PZT 40:60
PZT 30:70
PZT 20:80
PZT 10:90
PZT 0:100
Critical α (%)
ε_r of Buffer Layer
0
5
10
15
20
25
10
100

Figure 3